4674–4678 *Nucleic Acids Research, 1997, Vol. 25, No. 22*

Peptide nucleic acid–anthraquinone conjugates: strand invasion and photoinduced cleavage of duplex DNA

Bruce Armitage, Troels Koch[1], Henrik Frydenlund[1], Henrik Ørum[1], Hans-Georg Batz[2] and Gary B. Schuster*

School of Chemistry and Biochemistry, Georgia Institute of Technology, Atlanta, GA 30332-0400, USA, [1]PNA Diagnostics A/S, Rønnegade 2, DK-2100 Copenhagen, Denmark and [2]Boehringer Mannheim GmbH, Bahnhofstraße G-15, Tützing, Germany

Received June 25, 1997; Revised and Accepted September 10, 1997

ABSTRACT

A bis-peptide nucleic acid (PNA)–anthraquinone imide (AQI) conjugate has been synthesized and shown to form strand invasion complexes with a duplex DNA target. The two arms of the bis-PNA each consist of five consecutive thymine residues and are linked by a flexible, hydrophilic spacer. Probing with potassium permanganate reveals that the bis-PNA complexes to duplex DNA at $A_5 \cdot T_5$ sites with local displacement of the T_5 DNA strand. The 5 bp sequence targeted by the PNA is the shortest strand invasion complex reported to date. Irradiation of the strand invasion complex results in asymmetric cleavage of the displaced strand, with more efficient cleavage at the 3′-end of the loop. This result indicates that the bis-PNA binds to the DNA such that the C-terminal T_5 sequence forms the strand invasion complex, leaving the N-terminal T_5 sequence to bind by triplex formation, thereby placing the AQI closer to the 3′-end of the displaced strand, consistent with the observed photocleavage pattern. The ability of the PNA to directly report its binding site by photoinduced cleavage could have significant utility in mapping the secondary and tertiary structure of nucleic acids.

INTRODUCTION

Peptide nucleic acids (PNA) are DNA/RNA analogs in which nucleobases are appended to a polypeptide backbone at regular intervals (1). PNA oligomers consisting of thymine and cytosine bases (i.e. homopyrimidine PNA) bind to duplex DNA specifically at homopurine·homopyrimidine tracts (1–3). Homopyrimidine DNA oligonucleotides recognize these same homopurine·homopyrimidine sequences forming a local triplex structure by hydrogen bonding in the major groove according to the Hoogsteen motif ($T \times A \cdot T$, $C^+ \times G \cdot C$) (4–6). Binding of homopyrimidine PNA to duplex DNA involves a more complex recognition process. In the first examples discovered one PNA strand displaces the homopyrimidine DNA strand, forming a PNA–DNA hybrid duplex according to Watson–Crick rules. A second PNA strand then binds to the PNA–DNA hybrid by Hoogsteen hydrogen bonding, resulting in a PNA_2–DNA triplex and a locally displaced DNA strand (7). The displaced strand within this 'strand invasion complex' (the D loop) is readily cleaved by single strand-specific cleavage agents such as S1 nuclease and potassium permanganate (1).

The 'second generation' of strand invading homopyrimidine PNA oligomers have the two PNA strands connected by a flexible hydrophilic linker (8,9). Association of a bis-PNA with a single strand of homopurine DNA gives a complex that is significantly more stable than one formed with two single PNA strands due to a more favorable entropy of reaction. Moreover, bis-PNA is especially effective at forming strand invasion complexes with duplex DNA. Consequently, these derivatives are able to recognize and bind to short pyrimidine sequences in DNA, thereby increasing their potential utility as diagnostic reagents and therapeutic agents.

Strand invasion by bis-PNA has been demonstrated by the hyperreactivity of thymine residues in the displaced DNA strand to potassium permanganate (9). Recently Nielsen and Matsudaira independently reported examination of bis-PNA derivatives having a metal chelating group covalently linked to their N-termini (2,3). Since these conjugates cleave the DNA strands in regions close to their expected binding sites, they are being considered for applications in gene mapping and in antisense technology. Additionally, Nielsen and co-workers reported sequence-selective cleavage of duplex DNA by a bis-PNA–manganese porphyrin conjugate (10). Herein we report preparation and examination of a bis-PNA agent that is linked covalently to an anthraquinone imide (AQI) (Scheme 1). This conjugate forms strand invasion complexes with duplex DNA and irradiation with near UV light leads to selective patterned cleavage of the displaced DNA strand at the PNA binding site.

MATERIALS AND METHODS

Synthesis of AQI–Gly

Anthraquinone-2,3-anhydride (50 mg, 0.17 mmol) and Boc-Gly-OH (33 mg, 0.19 mmol) were suspended in acetic acid (0.5 ml). (The Boc protecting group on the amino acid improves solubility

*To whom correspondence should be addressed. Tel: +1 404 894 3300; Fax: +1 404 894 7466; Email: gary.schuster@cos.gatech.edu

in acetic acid, but is cleaved under the reaction conditions.) The suspension was heated to 120°C, which dissolved the reactants. The solution was kept at 120°C for 3 h and then cooled to room temperature. Crystals precipitated from the brown solution on standing at room temperature overnight. The crystals were collected by filtration, then washed several times with ether and dried. Yield: 46 mg (81%). ^{1}H NMR (d_6-DMSO): 13.8–12.6 p.p.m. (broad, -COOH), 8.52 p.p.m. (s, 2H, AQ aromatic CH), 8.29–8.26 p.p.m. (m, 2H, AQ aromatic CH), 8.03–7.96 p.p.m. (m, 2H, AQ aromatic CH), 4.42 p.p.m. (s, 2H, Gly-CH_2).

Synthesis of bis-PNA–AQI

The PNA was synthesized according to literature procedures (11,12). AQI–Gly was added to the PNA N-terminus using the conditions for monomer coupling. After cleavage of the PNA from the solid support and deprotection of the nucleobases, the PNA was purified by reversed phase HPLC and analyzed by MALDI-TOF mass spectrometry: calculated, 3543.4; found, 3541.5.

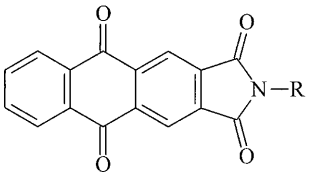

AQI

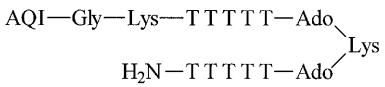

BisPNA-AQI

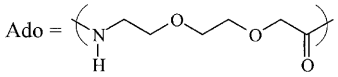

Scheme 1.

DNA labeling

For one set of experiments the 106 bp DNA restriction fragment obtained by digesting pUC19 plasmid DNA with *Afl*III and *Drd*I restriction enzymes was radioactively labeled at the unique *Afl*III site using [α-^{32}P]dCTP and the Klenow fragment of DNA polymerase. The labeled DNA was purified by electrophoresis through a 5% non-denaturing polyacrylamide gel followed by elution and ethanol precipitation, then used for the PNA binding and photocleavage experiments described below.

For other experiments 10 pmol synthetic DNA 25mer 5′-GCAAGCTACGTTTTTCGAGCTCGCA-3′ was labeled on the 5′-terminus using T4 polynucleotide kinase and [γ-^{32}P]ATP, then purified on a 20% denaturing polyacrylamide gel followed by elution and ethanol precipitation. A solution was then prepared containing ~20 nM labeled 25mer, 4.0 μM each unlabeled 25mer and the complementary strand (5′-TGCGAGCTCGAAAAACG-TAGCTTGC-3′) in 10 mM sodium phosphate buffer, pH 7.0, and heated to 75°C for 15 min, followed by slow cooling to room temperature to permit annealing of the DNA strands. The labeled DNA duplex was then used for the PNA binding and photocleavage experiments described below.

Strand invasion and photocleavage

bis-PNA–AQI was incubated with radiolabeled DNA at 37°C (for the restriction fragment) or 20°C (for the 25mer duplex) for 60 min to permit strand invasion. Samples were then used for permanganate probing of the thymine residues in the displaced strand or for photocleavage. In permanganate probing 0.5 μl 20 mM $KMnO_4$ was added to a 20 μl solution of strand invasion complex at room temperature. After 30 s 30 μl stop solution containing 5 μl 3 M sodium acetate, 2 μl 500 μM bp sonicated CT DNA, 1 μl β-mercaptoethanol and 22 μl water were added, followed by 100 μl cold ethanol. (In subsequent experiments β-mercaptoethanol was found to be unnecessary and was eliminated from the stop solution.) The DNA was precipitated, dried, then incubated with 100 μl 1 M piperidine at 90°C for 30 min in order to induce strand cleavage at the modified T residues.

For photocleavage experiments samples were irradiated using a Rayonet photoreactor equipped with $\lambda_{350\ nm}$ lamps. Samples of 20 μl were loaded into microcentrifuge tubes which were then suspended from a rotating platform inside the photoreactor. The irradiation time was adjusted to maintain 'single hit' conditions. After irradiation the samples were split into 2 × 10 μl aliquots which were then precipitated with ethanol and dried. One set of samples was then suspended in loading buffer while the other set of samples was treated with hot piperidine.

Permanganate cleavage and photocleavage were analyzed by separating the DNA fragments on denaturing polyacrylamide gels (10% for the restriction fragment, 20% for the 25 bp duplex) and autoradiography. The Maxam–Gilbert A+G reaction was used as a sequencing ladder in order to identify the cleavage sites.

RESULTS

bis-PNA–AQI (Scheme 1) was designed so that its two T_5 arms, linked by the flexible Ado–Lys–Ado group (Ado, 8-amino-3,6-dioxaoctanoic acid; Lys, L-lysine), will recognize and bind to $A_5{\cdot}T_5$ sequences in duplex DNA [Nielsen and co-workers used molecular modeling to determine that an Ado3 linker would provide sufficient length and flexibility to allow the two arms of a bis-PNA to bind a single strand of DNA (9). Ado–Lys–Ado was used in the present study in order to enhance DNA affinity due to the positively charged lysine residue]. Strand invasion and photocleavage experiments were performed on a 106 bp restriction fragment as well as a synthetic 25 bp duplex.

Restriction fragment

An appropriate target for bis-PNA–AQI is the 106 bp DNA restriction fragment obtained by digestion of pUC19 plasmid DNA with *Afl*III and *Drd*I. This fragment contains two $A_5{\cdot}T_5$ sequences that are separated by 16 bp and have opposite orientations (i.e. the A_5 sequences are located on opposite strands for the two sites). Thus, labeling the fragment using [α-^{32}P]dCTP and the Klenow fragment of DNA polymerase yields a DNA molecule having one $A_5{\cdot}T_5$ site with five adenines on the labeled strand and a second site with five thymines on the labeled strand. This arrangement permits simultaneous analysis of chemical

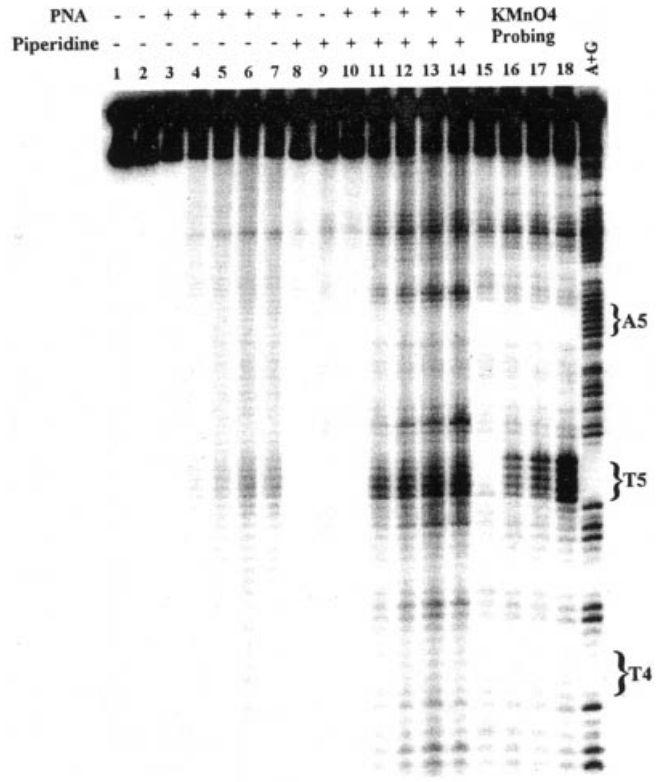

Figure 1. Autoradiogram demonstrating strand invasion and photocleavage by bis-PNA–AQI of a 106 bp restriction fragment. Potassium permanganate probes (lanes 15–18): lane 15, no PNA; lane 16; PNA; lanes 17 and 18, PNA + 100 μM bp CT DNA or 100 mM NaCl respectively added after formation of strand invasion complexes. Lanes 1–14, photocleavage; lanes 7 and 14 contained 100 μM bp CT DNA added after strand invasion but before irradiation. Irradiation times were 0 (lanes 1, 3, 8 and 10), 30 (lanes 4 and 11), 60 (lanes 5 and 12) and 120 min (lanes 2, 6, 7, 9, 13 and 14). Presence of PNA and treatment of the irradiated samples with hot piperidine are indicated above the lanes.

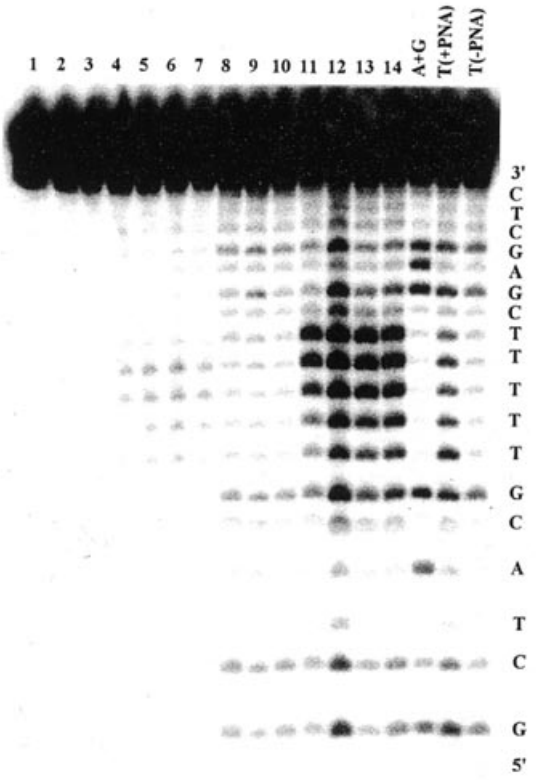

Figure 2. Autoradiogram demonstrating strand invasion and photocleavage by bis-PNA–AQI of a 25 bp DNA duplex. Potassium permanganate probing performed in the presence and absence of PNA (T lanes). Lanes 1–14, photocleavage; lanes 1, 2, 8 and 9 lacked PNA. Irradiation was performed for 0 (lanes 1, 3, 8 and 10), 15 (lanes 4 and 11), 30 (lanes 5 and 12), 45 (lanes 6 and 13) and 60 min (lanes 2, 7, 9 and 14). Lanes 8–14 were treated with hot piperidine prior to electrophoresis.

damage to the DNA on both the displaced and hybridized strands. Further, this DNA fragment also contains an $A_4 \cdot T_4$ sequence which provides data to assess the effect of a single mismatch on the recognition properties of bis-PNA–AQI.

Strand invasion by bis-PNA–AQI into duplex DNA was probed with potassium permanganate. Samples of the PNA and the target DNA were incubated for 1 h at 37°C prior to addition of permanganate. The permanganante reaction was quenched by addition of sodium acetate after 30 s to mimic the extent of the photochemical reaction described below. After treatment of the samples with hot piperidine high resolution PAGE shows no strand cleavage in the absence of bis-PNA–AQI (Fig. 1, lane 15). When the PNA is present cleavage at the T_5 site is readily detected and each thymine at this site is cleaved with the same efficiency by permanganate (Fig. 1, lane 16). This result provides clear evidence for strand invasion by the PNA. To test the stability of the PNA–DNA complex this experiment was repeated on a sample containing excess calf thymus DNA that was added to the solution after complex formation. The excess DNA has no effect on permanganate cleavage (Fig. 1, lane 17), demonstrating the kinetic stability of this complex and confirming the remarkably slow off-rates for bis-PNA reported by Griffith and co-workers (8). Significantly, complete absence of permanganate-induced cleavage at the T_4 site demonstrates the high degree of sequence selectivity for strand invasion by bis-PNA–AQI. [The observation that 100 mM NaCl significantly enhances permanganate hyperreactivity (lane 18) is attributed to screening of charge repulsion between the permanganate and DNA by the sodium cations.] Finally, inclusion of 100 mM NaCl in the reaction buffer leads to strong enhancement of permanganate reactivity of the D loop (lane 18), however, rather than being due to improved strand invasion by the PNA at higher salt concentration, it is likely that the added sodium cations help to screen electrostatic repulsion between the DNA and the permanganate, both of which bear negative charges.

Irradiation of the PNA–DNA complexes results in weak spontaneous (i.e. no alkali treatment) background cleavage at all positions (i.e. sequence-neutral) as well as enhanced cleavage at the T_5 site (Fig. 1, lanes 4–7). Importantly, no such enhancement is observed at the A_5 site, indicating that the AQI reacts more efficiently with the displaced strand within the complex. Spontaneous sequence-neutral cleavage is characteristic of AQI derivatives, where strand scission is proposed to result from quinones which are bound to DNA and react by photoinduced hydrogen atom abstraction from a deoxyribose (13). The observation that this background cleavage is unaffected by excess

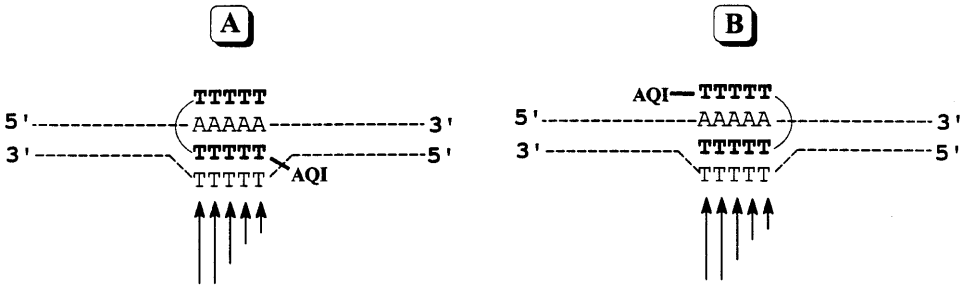

Figure 3. Possible orientations of bis-PNA–AQI within strand invasion complexes. Because of the symmetrical recognition sequence, either arm of the bis-PNA can act as the invading strand, leaving the other arm to form the local triplex. In Model A the five T bases at the N-terminus of the PNA displace the homopyrimidine DNA strand, while the C-terminal arm forms the triplex. This orientation directs the AQI toward the 5′-end of the displaced strand. The roles for the two arms are reversed in Model B, resulting in orientation of the AQI toward the 3′-end of the displaced strand. The arrows represent the approximate amount of cleavage observed at each base.

CT DNA (compare lane 7 with lane 6) shows that this damage is not due to a freely diffusing reagent but rather to a non-selectively bound PNA–AQI conjugate. (The strand invasion complex was formed in the presence of excess bis-PNA–AQI. The two positive charges on the PNA as well as the AQI moiety will promote non-selective binding to the DNA. However, the results of the permanganate hyperreactivity experiment clearly demonstrate that strand invasion occurs specifically at the target sequence.)

Piperidine treatment of the irradiated complex results in a substantial increase in the yield of cleavage at the D loop T_5 site, while the A_5 site remains unaffected (Fig. 1, lanes 11–14). [The additional cleavage bands observed in lanes 11–14 correspond to the 5′-Gs of GG steps. Cleavage at these sites is attributed to electron transfer from the DNA bases to the AQI followed by migration of the hole to the GG site, where it is trapped by water and/or oxygen. This is a surprising finding because untethered AQI fails to cleave DNA by this mechanism (9), suggesting that the GG cleavage observed for bis-PNA–AQI arises from the strand invasion complexes, in which case hole migration is absolutely required in order to account for the observed cleavage at remote GG sites (for GG-selective cleavage by other AQ derivatives see 14,15). Of particular interest is the distinct asymmetry in the pattern at the T_5 site: the thymines at the 3′-end of the D loop are cleaved significantly more efficiently than are those at the 5′-end. This asymmetry is in distinct contrast to the cleavage reported for bis-PNA–metal chelator conjugates, in which cleavage was favored at the 5′-end of the D loop when the chelator is tethered to the bis-PNA at the N-terminus (2,3). The light-induced cleavage asymmetry contrasts with the uniform cleavage pattern arising from permanganate oxidation, indicating that the 3′-end preference for photocleavage in the loop is not due to asymmetry within the loop itself but rather to accessibility of the AQI to the sites, determined by the structure of the strand invasion complex.

Synthetic 25mer duplex

A 25 bp duplex was designed which contained a single recognition site for the bis-PNA. The T_5-containing strand was radiolabeled at the 5′-terminus and hybridized with a >200-fold excess of unlabeled complement. The DNA duplex was then incubated with an equimolar amount of bis-PNA–AQI (relative to unlabeled DNA) at 20°C for 60 min to permit strand invasion. This temperature was selected because thermal denaturation experiments reveal that the complex formed by bis-PNA–AQI and just the T_5-containing 25mer melts at ~40°C.

Probing the synthetic DNA duplex with permanganate reveals that strand invasion occurs, since cleavage is observed at each of the five thymine residues at the recognition site (Fig. 2, compare lanes T+PNA and T–PNA). Irradiation of the strand invasion complex reveals a low level of spontaneous cleavage also at the T_5 site (lanes 4–7). As with the restriction fragment, piperidine treatment significantly enhances cleavage at these sites, but gives very little damage outside the target region. Again, this procedure shows a preference for cleavage at the 3′-end of the recognition site, even though a uniform cleavage pattern is observed when this structure is treated with permanganate.

DISCUSSION

Watson–Crick recognition of DNA by PNA generally yields duplexes in which the PNA strand is oriented with the N→C direction antiparallel to the DNA 5′→3′ direction (16). Because of the sequence symmetry of the DNA targeted in the restriction fragment examined here there are two possible structures for the strand invasion complex (Fig. 3). In both cases the PNA Watson–Crick strand is oriented antiparallel to the homopurine DNA tract, while the Hoogsteen strand is parallel. A significant difference between the two structures is the position of the AQI with respect to the D loop: in structure A the quinone is positioned at the 5′-end of the loop, while in B it is placed closer to the 3′-end. Model B is the more appealing based on two considerations: (i) the quinone causes less perturbation to the DNA because it is tethered to the arm of the PNA which is not involved in strand invasion; (ii) this model places the AQI closer to the terminus at which cleavage is most efficient. However, the possibility that both complexes are formed but only one leads to photocleavage cannot be ruled out. Future work on conjugates with longer linking groups between the AQI and the PNA as well as DNA targets with asymmetrical recognition sites will further clarify the structure of the bis-PNA–AQI/DNA strand invasion complexes.

It is interesting to compare photocleavage by the AQI chromophore in the bis-PNA–AQI/DNA strand invasion complexes with the results of oxidative cleavage by a bis-PNA–porphyrin conjugate. In the porphyrin case the strongest cleavage sites do not occur within the displaced strand but rather at the junction between the duplex DNA and the strand invasion complex, a feature which is attributed to preferential association of the porphyrin with the DNA outside the strand invasion complex. On the other hand,

photocleavage by the anthraquinone is highly selective for the displaced strand, suggesting that the AQI loops back and preferentially associates with the strand invasion complex, rather than simply extending along one of the grooves of the DNA. The linker lengths are similar in the two cases (seven bonds for the porphyrin, six bonds for the AQI), but the linker in the AQI case includes a positively charged lysine residue while the linker for the porphyrin is an uncharged alkyl chain. Variation of linker length and charge could lead to significant effects on the cleavage sites by bis-PNA-linked nucleases.

In conclusion, conjugation of AQI to a bis-PNA yields a compound which effectively combines the DNA recognition properties of PNA with the photonuclease properties of the anthraquinone chromophore. Both permanganate hyperreactivity and photoinduced cleavage of the DNA by bis-PNA–AQI clearly demonstrate strand invasion by the PNA, with no tolerance for a single mismatch within the recognition sequence. The 5 bp recognition site represents the shortest sequence successfully targeted by PNA without loss of specificity. The complexed DNA strand is not cleaved by the AQI within the strand invasion complex. The ability of the PNA to directly report on its binding site by patterned photoinduced cleavage could have significant utility when the looped strand is inaccessible to external reagents, such as in nucleic acids which possess significant tertiary structure.

ACKNOWLEDGEMENT

This work was supported by funding from the National Institutes of Health (PHS NRSA GM16498-01 to B.A. and grant RO1 GM28190 to G.B.S.), for which we are grateful.

REFERENCES

1 Nielsen,P.E., Egholm,M., Berg,R.H. and Buchardt,O. (1991) *Science*, **254**, 1497–1500.
2 Footer,M., Egholm,M., Kron,S., Coull,J.M. and Matsudaira,P. (1996) *Biochemistry*, **35**, 10673–10679.
3 Lohse,J., Hui,C., Sönnichsen,S.H. and Nielsen,P.E. (1996) In Meunier,B. (ed.), *DNA and RNA Cleavers and Chemotherapy of Cancer and Viral Diseases*. Kluwer Academic Publishers, Dordrecht, The Netherlands, pp. 133–141.
4 Frank-Kamanetskii,M.D. and Mirkin,S.M. (1995) *Annu. Rev. Biochem.*, **64**, 65–96.
5 Le Doan,T., Perrouault,L., Praseuth,D., Habhoub,N., Decout,J.L., Thuong,N.T., Lhomme,J. and Hélène,C. (1987) *Nucleic Acids Res.*, **15**, 7749.
6 Moser,H.E. and Dervan,P.B. (1987) *Science*, **238**, 645–650.
7 Demidov,V.V., Yavnilovich,M.V., Belotserkovskii,B.P., Frank-Kamenetskii,M.D. and Nielsen,P.E. (1995) *Proc. Natl. Acad. Sci. USA*, **92**, 2637–2641.
8 Griffith,M.C., Risen,L.M., Greig,M.J., Lesnik,E.A., Sprankle,K.G., Griffey,R.H., Kiely,J.S. and Freier,S.M. (1995) *J. Am. Chem. Soc.*, **117**, 831–832.
9 Egholm,M., Christensen,L., Dueholm,K.L., Buchardt,O., Coull,J. and Nielsen,P.E. (1995) *Nucleic Acids Res.*, **23**, 217–222.
10 Bigey,P., Sönnichsen,S.H., Meunier,B. and Nielsen,P.E. (1997) *Bioconjugate Chem.*, **8**, 267–270.
11 Christensen,L., Fitzpatrick,R., Gildea,B., Petersen,K.H., Hansen,H.F., Koch,T., Egholm,M., Buchardt,O., Nielsen,P.E., Coull,J. and Berg,R.H. (1995) *J. Peptide Sci.*, **3**, 175–183.
12 Koch,T., Hansen,H.F., Andersen,P., Larsen,T., Batz,H.G., Ottesen,K. and Ørum,H. (1997) *J. Peptide Res.*, **49**, 80–88.
13 Breslin,D.T., Coury,J.E., Anderson,J.R., McFail-Isom,L., Kan,Y., Williams,L.D., Bottoley,L.A. and Schuster,G.B. (1997) *J. Am. Chem. Soc.*, **119**, 5034–5044.
14 Breslin,D.T. and Schuster,G.B. (1996) *J. Am. Chem. Soc.*, **118**, 2311–2319.
15 Ly,D., Kan,Y., Armitage,B. and Schuster,G.B. (1996) *J. Am. Chem. Soc.*, **118**, 8747–8748.
16 Egholm,M., Buchardt,O., Christensen,L., Behrens,C., Freier,S.M., Driver,D.A., Berg,R.H., Kim,S.K., Nordén,B. and Nielsen,P.E. (1993) *Nature*, **365**, 566–568.